THE ANNALS OF "DUNAREA DE JOS" UNIVERSITY OF GALATI.
FASCICLE IX. METALLURGY AND MATERIALS SCIENCE
N^0. 1 – 2009, ISSN 1453 – 083X

ELEMENTS OF DRAWING THEORY AND TECHNOLOGY OF THE HIGH MECHANICAL STRENGTH WIRES IN ULTRASONIC FIELD

Viorel ILIESCU[1], Mihai SUSAN[2], Roxana Gabriela ŞTEFANICĂ[2], Dragoş Cristian ACHIŢEI[2], Brian Tudor LANDKRAMMER[2]
[1]SC CABLERO SA Iaşi,
[2]Gheorghe Asachi Technical University of Iaşi, Faculty of Material Science and Engineering
email: mihaisusan@yahoo.com

ABSTRACT

In the paper are presented elements of drawing theory and technology of the high mechanical strength wires, when the auger die is located in the maximum of the waves oscillation and it is activated on drawing direction. Force parameters are determined based on the theorem of total consumed power considering metal-tool friction Coulomb type. In order to form a stable system of stationary waves into processed wire there are used ultrasonic energy reflectors. The experiments are accomplished in laboratory on wires made of RUL 1V/ AISI 52100.

KEYWORDS: drawing, wire, ultrasonic field, force parameters, ultrasonic energy reflectors, mechanical characteristics of resistance and plasticity.

1. Introduction

The wires/metallic wires are generally obtained through cold drawing. The plastic deformation through cold drawing is accompanied by cold-hardenings of cold-age hardening which complicates the plastic deformation for great reduction degrees of the section of the blank wire. The cold-hardening is much more obvious for metallic wires of high mechanical resistance. In the present paper is presented their processing in ultrasonic field "ultrasonic vibration drawing-UVD" or UVD technology, as an alternative to the classical technology (CT).

The characterization of the UVD technology compared to the classical technology (CT) is realized on two objective directions such as:

(i) the calculus of the force parameters;

(ii) the efficiency of the UVD technology.

2. The calculus of force parameters

The calculus of force parameters is made taking into consideration the deformation zone of the material, the ball-shaped rate field and the Bernoulli type laminar flow, figure 1.

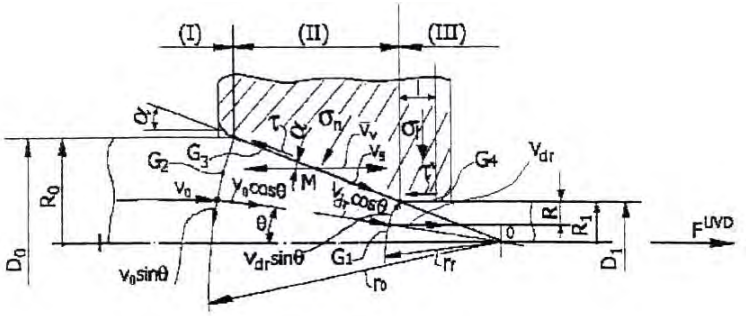

Fig.1. *The interior geometry of the auger die and the components of the rate in the deformation zone of the material [1].*

2.1. The rate field at wire drawing

The hypotheses of plastic deformation are: the metallic material is incompressible, the auger die is a rigid body and the metal deformation occurs according to Von Mises flow condition, the Coulomb type metal-tool contact friction, on the oscillating system only longitudinal elastic waves are acting in stationary regime and the deformation process is isothermal, [1, 2].

In the areas (I) and (III) the rate is uniform and has only axial components with the values v_0 and v_{tr} existing the interdependency relationship:

$$v_0 = v_{tr}(R_1/R_0)^2 \tag{1}$$

The area of plastic deformation (II) is bounded by two spherical surfaces; G_1 of radius r_f and G_2 of radius r_0 and by a conic surface G_3 (defined by the taper opening of the auger die 2α). In this area the rate is oriented towards the cone's tip, 0, having cylindrical symmetry. In spherical coordinates (r, θ, φ) the components of the displacement rate are determined as displacement derivatives as a function of time $\dot{u}_r, \dot{u}_\theta$ and $\dot{u}_\varphi$. The components of the deformation rate are determined as derivatives of the deformation degree as a function of time and are presented in [2].

The components of displacement rate in (II) zone are:

$$\begin{cases} \dot{u}_r = v = -v_{tr}\cdot r_f{}^2(\cos\theta/r_0{}^2) \\ \dot{u}_0 = \dot{u}_\varphi = 0 \end{cases} \tag{2}$$

Along the G_1 and G_2 limits, the normal components of the rate are continuous; however rate discontinuities occur at parallel positions to these limits:

- for G_1: $\Delta v_1 = v_{tr}\cdot\sin\theta$
- for G_2: $\Delta v_2 = v_0\cdot\sin\theta$ (3)

It appears rate discontinuities both on the conic surface G_3 and on cylindrical surface G_4 since the auger die is a rigid body:

- for G_3: $\Delta v_3 = v_{tr}\cdot r_f{}^2(\cos\alpha/r_0{}^2)$
- for G_4: $\Delta v_4 = v_{tr}$ (4)

Under these circumstances, the volumetric rate $\dot{V}$ of metal flow through any surface bounded by the conical tubular channel defined by dθ ise identical to the rate of metal flow through the elementary tube defined by dR. Therefore, in zone (III):

$$R = r_f\cdot\sin\theta; dR = r_f\cdot\cos\theta\cdot d\theta;$$

$$\dot{V}_3 = 2\pi R\cdot dR\cdot v_{tr} = \tag{5}$$
$$= 2\pi\cdot v_{tr}\cdot\sin\theta\cdot\cos\theta\cdot d\theta$$

In zone (II): $\dot{V}_2 = -2\pi r\cdot\sin\theta\cdot r\cdot d\theta\cdot\dot{u}_r$ (6)

From the congruency of the two volumetric rates it results:

$$\dot{u}_r = -v_{tr}\cdot r_f{}^2(\cos\theta/r_0{}^2) \tag{7}$$

2.2. The consumed power through drawing

According to the theorem of the total consumed power it can be written the congruency:

$$\dot{W}_{tot} = \dot{W}_{def} + \dot{W}_{SG} \tag{8}$$

The necessary power for plastic deformation by drawing has the expression:

$$\dot{W}_{nec} = \pi\cdot v_{tr}\cdot R_1{}^2\cdot\sigma^{UVD} \tag{9}$$

σ^{UVD} - should balance the total consumption of power.

2.2.1. The consumed power for the proper plastic deformation

It can be noticed from figure 1 that in the areas (I) and (III) it is not produced the plastic deformation of the metal.

The plastic deformation of the metal occurs only in the area (II).

Owing to the axial-cylindrical symmetry as a function of φ, equation system becomes:

$$\begin{cases} \dot{\varepsilon}_{rr} = \partial\dot{u}_r/\partial r \\ \dot{\varepsilon}_{\theta\theta} = \dot{u}_r/r \\ \dot{\varepsilon}_{\varphi\varphi} = \dot{u}_r/r \\ \dot{\varepsilon}_{r\theta} = (1/2r)\cdot\left(\partial\dot{u}_r/\partial\theta\right) \\ \dot{\varepsilon}_{\theta\varphi} = \dot{\varepsilon}_{r\varphi} = 0 \end{cases} \tag{10}$$

Considering the rate field equations given by relationship (4) the deformation rates become:

$$\begin{cases} \dot{\varepsilon}_{rr} = -2\dot{\varepsilon}_{\theta\theta} = -2\dot{\varepsilon}_{\varphi\varphi} = 2v_{tr}\cdot\dot{r}_f{}^2(\cos\theta/r_0{}^3) \\ \dot{\varepsilon}_{r\theta} = (1/2)\cdot v_{tr}\cdot\dot{r}_f{}^2(\sin\theta/r_0{}^3) \\ \dot{\varepsilon}_{\theta\varphi} = \dot{\varepsilon}_{r\varphi} = 0 \end{cases} \tag{11}$$

So that the consumed power for proper deformation has the expression:

$$\dot{W}_{def} = (2/\sqrt{3})\sigma_c\cdot\int_V\sqrt{(1/2)(\dot{\varepsilon}_{ij}\cdot\dot{\varepsilon}_{ji})}\cdot dV \tag{12}$$

or

$$\dot{W}_{def} = (2/\sqrt{3})\sigma_c\int_V v_{tr}\cdot\dot{r}_f{}^2(1/r^3)\sqrt{3\cos^2\theta + (1/4)\sin^2\theta}\cdot dV =$$
$$= 2\sigma_r\cdot v_{tr}\cdot\dot{r}_f{}^2\cdot\int_V(1/r^3)\sqrt{1-(11/12)\sin^2\theta}\cdot dV \tag{13}$$

where:

$$dV = 2\pi r \cdot \sin\theta \cdot r \cdot d\theta \cdot dr \qquad (14)$$

Replacing dV into relationship (15) it is obtained the new relationship for $\dot{W}_{def}$:

$$\dot{W}_{def} = 4\pi\sigma_c \cdot v_{tr} \cdot r_f^2 \cdot \int_{\theta=0}^{\alpha}\left[\sqrt{1-\frac{11}{12}\cdot\sin^2\theta}\cdot\sin\theta\cdot\int_{r=r_f}^{r_0}\frac{dr}{r}\right] = 4\pi\sigma_c \cdot v_{tr} \cdot r_f^2 \cdot \ln\left(\frac{r_0}{r_f}\right)\cdot\int_{\theta=0}^{\alpha}\left[\sqrt{1-\frac{11}{12}\cdot\sin^2\theta}\cdot\sin\theta\cdot d\theta\right] \qquad (15)$$

After integration it results the expression:

$$\dot{W}_{def} = 2\pi\sigma_c \cdot v_{tr} \cdot r_f^2[1-\cos\alpha\sqrt{1-(11/12)\sin^2\alpha}+\frac{1-(11/12)}{\sqrt{11/12}}\cdot\ln\frac{1+\sqrt{11/12}}{(\sqrt{(11/12)}\cdot\cos\alpha+\sqrt{1-(11/12)\cdot\sin^2\alpha}}]\cdot\ln(r_0/r_f) \qquad (16)$$

Taking into consideration the fact that:

$r_0 / r_f = R_0 / R_1$ and $r_f = R_1(1/\sin\alpha)$

It results:

$$\dot{W}_{def} = 2\pi\sigma_c \cdot v_{tr} \cdot R_1^2 \cdot f(\alpha)\cdot\ln(R_0/R_1) \qquad (17)$$

where:

$$f(\alpha) = (1/2\sin^2\alpha)[1-\cos\alpha\sqrt{1-(11/12)\sin^2\alpha}+\frac{1}{\sqrt{11\cdot12}}\cdot\ln\frac{1+\sqrt{11/12}}{(\sqrt{11/12})\cdot\cos\alpha+\sqrt{1-(11/12)\cdot\sin^2\alpha}} \qquad (18)$$

n smaller angles f(α) tend to unity and the relationship (19) becomes:

$$\dot{W}_{def} = 2\pi\sigma_c \cdot v_{tr} \cdot R_1 \cdot \ln(R_0/R_1) \qquad (19)$$

The latest relationship is considered to be the definition of the ideal power for a uniform rate field:

$$u_r = v = -v_{tr}(r_f^2 / r_0) \qquad (20)$$

2.2.2. The lost power caused to the rate discontinuities

As it is noticed in figure 1 the G_1 and G_2 surfaces are surfaces of rate discontinuities. The metal discharge is the same no matter if is calculated with relationships that describe the rate field to the right or to the left of these surfaces.

The condition of metal flow continuity requires the normal components of the rate, derived from each of the rate field on these surfaces, to be equivalent. So that, for the G_1 surface, the normal component to the left has the expression:

$$\left|\dot{u}_r\right| = v_{tr}\cdot\cos\theta \qquad (21)$$

Analogous by the axial component of the rate v_{tr} of the zone (III), normal on the G_1 surface is equal with $v_{tr}\cdot\cos\alpha$.

The tangential components are no longer equal, the difference is known also as rate discontinuity.

Based on Von Mises flowing criterion, the power consumed along the G_1 and G_2 surfaces has the expression:

$$\dot{W}_{SG_1,G_2} = \int_{G_1G_2}\tau\cdot\Delta v\cdot dS = \int_{G_1}\tau\cdot\Delta v_1\cdot dS + \int_{G_2}\tau\cdot\Delta v_2\cdot dS = 4\pi\cdot v_{tr}\cdot r_f^2(\sigma_c/\sqrt{3})\int_{\theta=0}^{\alpha}\sin^2\theta\cdot d\theta \qquad (22)$$

after integration $\dot{W}_{SG_1G_2}$ becomes:

$$\dot{W}_{SG_1G_2} = (2/\sqrt{3})\sigma_c\cdot\pi\cdot v_{tr}\cdot r_f^2(\alpha-\sin\alpha\cdot\cos\alpha) = (2/\sqrt{3})\sigma_c\cdot\pi\cdot v_{tr}\cdot R_1^2[(\alpha/\sin^2\alpha)-\mathrm{ctg}\alpha] \qquad (23)$$

2.2.3. The consumed power caused by friction losses

The power losses caused by metal-tool friction are consumed at the level of G_3 and G_4 surfaces.

Along the conical portion, bounded by G_3 surface (figure 1), the rate discontinuity is given by the relationship:

$$\Delta v_3 = v_{tr}(r_f^2/r_0^2)\cos\alpha = v_{tr}(R_1/R_0)^2\cdot\cos\alpha \qquad (24)$$

and the contact surface element is:

$$dS = 2\pi R(dR/\sin\alpha) \qquad (25)$$

Up to the cylindrical surface G_4 the rate discontinuity is $\Delta v_4 = v_{tr}$.

Taking into consideration the expression given by Sach's relationship for σ_r [3]:

$$\sigma_r = \sigma_c[\ln(R_0/R_1)^2 - 1] \qquad (26)$$

It results the expressions for the friction losses:

$$\dot{W}_{SG_3} = \int_{G_3}\tau\cdot\Delta v_3\cdot dS = 2\pi\cdot\mu^{UVD}\cdot v_{tr}\cdot R_1^2\cdot ctg\alpha[1-\ln(R_0/R_1)]\sigma_c\cdot\ln(R_0/R_1) \quad \text{and:}$$

$$W_{SG_4} = \tau \cdot \Delta v_4 \cdot dS = 2\pi \cdot \mu^{UVD} \cdot v_{tr} \cdot R_1^2 \cdot (l / R_1)(\sigma_c - \sigma^{UVD}) \quad (27)$$

In relationships (27) and (28) the friction factor μ^{UVD} is determined with the relationship [3]:

$$\mu^{UVD} = \mu^{CT}(1 - \frac{2}{\pi}\arccos\frac{v_{tr}}{v_0}) \quad (28)$$

with $\left|v_{tr} / \overline{v_0}\right| \le 1{,}0$.

The drawing stress (σ^{UVD}) is determined with relationship (32).

2.2.4. The drawing stress and force

From the made power balance it results for the classical technology, the following drawing stress (noted σ^{CT}):

$$\sigma^{CT} = \sigma_c\{2f(\alpha)\cdot\ln(R_0/R_1) + 2/\sqrt{3}[(\alpha/\sin^2\alpha) - \mathrm{ctg}\alpha] + 2\mu^{CT}[\mathrm{ctg}\alpha(1-\ln(R_0/R_1))]\cdot\ln(R_o/R_1) + 1/R_1]\}/[1+2\mu^{CT}(l/R_1)] \quad (29)$$

Coincidently the drawing force (F^{CT}) has the expression:

$$F^{CT} = S_1 \cdot \sigma^{CT} = \frac{1}{4}\cdot\pi\cdot D_1^2\cdot\sigma^{CT} \quad (30)$$

For the UVD technology the drawing stress (σ^{UVD}) has the expression:

$$\sigma^{UVD} = \sigma_c\{2f(\alpha)\cdot\ln(R_0/R_1) + 2/\sqrt{3}[(\alpha/\sin^2\alpha) - \mathrm{ctg}\alpha] + [\mathrm{ctg}\alpha(1-\ln(R_0/R_1))]\cdot\ln(R_0/R_1) + 1/R_1]\cdot\frac{2\mu^{UVD}}{1+\frac{R_0}{R_1}\mu^{UVD}} \quad (31)$$

The drawing force for the UVD technology is determined with the relationship:

$$F^{UVD} = \frac{1}{4}\pi D_1^2\cdot\sigma^{UVD} \quad (32)$$

3. Experimental procedure

The experiments were performed on a classical hydraulically actuated drawing bench able to develop a drawing force of $12\cdot10^4$ N and an active stroke of 1,5 m. the assembly of the oscillating system has been fastened on the resistance frame of the bench by means of the nodal flange.

The principle scheme of the experimental installation, used for wire drawing in ultrasonic field is illustrated in fig. 2, [4].

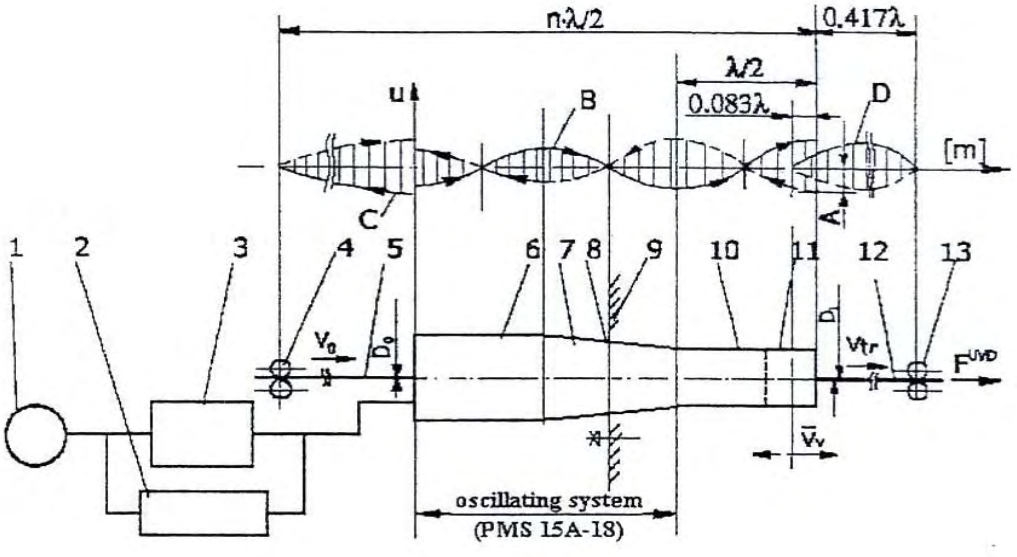

Fig.2. *Principle scheme of the experimental installation used for wire drawing in ultrasonic field, according to UVD technology: 1 – supply bloc; 2 – polarization bloc; 3 – ultrasonic generator type UZG 2-4M; 4, 13 – reflectors of ultrasonic energy (pressure rolls); 5 – raw wire; 6 – magnetostrictive transducer; 7 – conical concentrator; 8 – nodal flange; 9 – frame of the classical drawing device; 10 – guide for ultrasonic waves; 11 – die; 12 – processed wire; A – amplitude of die's oscillations; B – wave oscillation in processed wire; ——— progressive wire; ------- regressive wave, [4,5].*

The UZG 2-4M type ultrasonic generator, with a power of 2000 W and resonance frequency f = $17{,}5\cdot10^3$ Hz, works in conjunction with the PMS 15A-18 type oscillating system, which comprises a magnetostrictive transducer and a conical wave concentrator made from titanium based alloy. At the right side of the conical concentrator a guiding device core and convergent conical inner geometry with semi angle conicity $\alpha = 8°$ and cylindrical calibration zone. As drawing lubricant soap powder was used in a mixture with 10-15% fine lime powder and 12-15% tale powder. The assembly of the oscillating system is dimensioned as a multiple of $\lambda/2$, where $\lambda = c / f$ - is the ultrasonic wave length determined by the ultrasonic propagation rate (c) in the metallic wire and resonance frequency (f).

The ultra-acoustic energy reflectors (pressure rolls) play the role to limit the action of ultrasonic energy upon well defined portions of both raw and processed wire, from AISI 52100 (RUL IV / STAS 11250) ball bearing steel.

Raw wire had initial diameter $D_0 = 4{,}6\cdot10^{-3}$ m and the chemical composition : Fe - 1.2C - 0.4Mn – 0.3Si – 0.5Cr – 0.02S – 0.02P - 0.08Mo – 0.2Ni – 0.2Cu (wt%). The wire was processed by single stage drawing to the final diameter $D_1 = 4.22\cdot10^{-3}$ m.

The mechanical characteristics of resistance (yield stress, $R_{p0.2}$, and tensile strength, R_m) and plasticity (ultimate strain, A_5), were determined, for both raw and drawn wires, by tensile tests performed, according to EN 10002-1/1995, with a strain rate of $3.33\cdot10^{-4}$ m/sec, on MTS 810.24 tensile testing machine.

4. Experimental results and discussion

In the case of classical technology (CT), the experimental average value of the drawing force was determined as $F_{ex}^{CT} = 1370\ N$. With this value, the experimental values were calculated for the drawing stress, $\sigma_{ex}^{CT} = 98\ MPa$, by means of means of relationship (32) and for the friction coefficient μ^{CT} 0.026, by means of Sach's relationship given in [3]. The effects of ultrasonic oscillation amplitude on both technological parameters and efficiency of UVD technology are summarized in table 1.

Table 1. *Effects of ultrasonic amplitude on bloth the technological parameters and the efficiency of the UVD technology in case of processing AISI 52100 ball bearing steel wires*

Ultrasonic oscillation amplitude at UVD technology	Technological parameters				UVD efficiency
	$v_{tr}/\bar{v}_v$ -	μ^{UVD} -	F_{an}^{UVD} [N]	F_{ex}^{UVD} [N]	ΔF [%]
$5\cdot10^{-6}$ m	0.54	0.0062	1259	1250	8.75
$15\cdot10^{-6}$ m	0.18	0.0044	1205	1184	13.57
$20\cdot10^{-6}$ m	0.13	0.0030	1179	1147	16.27

Based on the value of the friction coefficient for classical technology, $\mu^{CT} = 0.026$, in column 3 the friction coefficients at UVD technology , μ^{UVD}, were calculated as a function of relative deformation rates $v_{tr}/\bar{v}_v$, by means of relationship (28). As compared to classical technology (CT) values at least four times lower were obviously obtained for UVD technology.

The values of the analytical drawing force at UVD technology, F_{an}^{UVD}, were calculated in column 4 with relationship (32), based on the analytical drawing stress at UVD technology , σ_{an}^{UVD} determined with (31), where l is length of the calibration zone of the die. Column 5 lists the experimental values with the analytical ones.

Finally, the efficiency of the UVD technology compared to CT was determined in column 6 with relationship: $\Delta F = 100\cdot\left[1-\left(F_{ex}^{UVD}/F_{ex}^{CT}\right)\right]$.

It is obvious that this highest efficiency was obtained for the ultrasonic oscillation amplitude A = $20\cdot10^{-6}$ m, which gives the lowest relative deformation rate, in agreement with our previous observations [4, 5].

The tensile – strain curves, determined as average values of five tests performed on raw (annealed) wires, on wires drawn with CT and on the three sets of wires processed by UVD are illustrated in fig. 3.

On one hand, in case of CT, designated by 0 oscillation amplitude, the drawn wires were obviously work hardened as compared to raw (annealed) wires.

On the other hand, it is noticeable that, with the increase of ultrasonic oscillation amplitude, the decrease of intensity of the work hardening phenomenon in ultrasonically drawn wires occurs, which causes low mechanical characteristics of resistance and higher plasticity as shown in table 2.

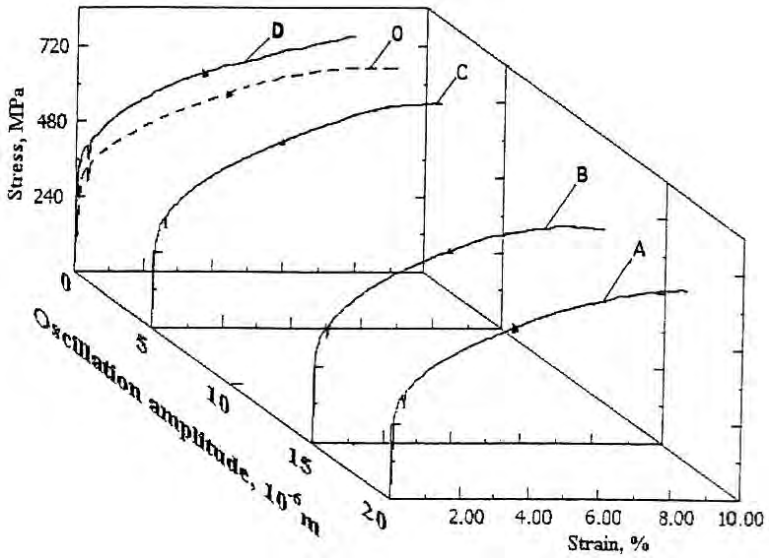

Fig.3. *Influence of the oscillation amplitude of ultrasonic at UVD technology on the tensile stress-strain curves of processed wires.*

Table 2. *Yield stress, ($R_{p0.2}$), tensile strength, (R_m) and ultimate strain, (A_5) of the curves from fig.3*

A, 10^{-6} m	0		5	15	20
	raw wire	CT	UVD		
$R_{p0.2}$ [MPa]	332	401	370	349	327
R_m [MPa]	650	746	711	685	667
A_5 [%]	9.15	7.87	8.01	8.38	8.46

5. Conclusions

Based on a rate field with spherical distribution, a relationship was established for the drawing force for the metal wires and the analytical values were in very good agreement with the experimental ones, determined at UVD processing of AISI 52100 (RUL IV/ STAS 11250) ball bearing steel wires.

With increasing ultrasonic oscillation amplitude applied to the die, from 5 to 20 · 10^{-6} m, progressive decreases were obtained for both the drawing force, from 1250 to 1147 N, and the friction coefficient, from 0.0062 to 0.003. As compared to classical technology, efficiency higher that 16% were obtained for UVD technology. By tensile tests it was emphasised that UVD technology not only allows lower drawing forces but also reduces the works hardening level – a phenomenon which is always present in classical technology – causing increases of ultimate strain from 7.87% at CT to 8.46%.

References

[1]. Susan, M. - *Trefilarea sârmelor de oţel.* Editura CERMI, Iaşi, 2008.
[2]. Cazimirovici, E. ş.a. - *Teoria şi tehnologia deformării plastice prin tragere,* Editura Tehnică, Bucureşti, 1990.
[3]. Susan, M., s.a. - *On the drawing in ultrasonic field of metallic wires high mechanical resistance.* Journal of Optoelectronic and Advanced Materials, 7(2), Aprilie, pp. 637-645, 2005
[4]. *** Contract CNCSIS - tip A, GR 63 – 23.05.2006.
[5]. *** Contract CNCSIS - tip A, GR 80 – 23.05.2007.